

# Progress on “pico” air vehicles

R.J. Wood, B. Finio, M. Karpelson, K. Ma, N.O. Pérez-Arancibia, P.S. Sreetharan, H. Tanaka, and J.P. Whitney

**Abstract** As the characteristic size of a flying robot decreases, the challenges for successful flight revert to basic questions of fabrication, actuation, fluid mechanics, stabilization, and power - whereas such questions have in general been answered for larger aircraft. When developing a flying robot on the scale of a common housefly, all hardware must be developed from scratch as there is nothing “off-the-shelf” which can be used for mechanisms, sensors, or computation that would satisfy the extreme mass and power limitations. This technology void also applies to techniques available for fabrication and assembly of the aeromechanical components: the scale and complexity of the mechanical features requires new ways to design and prototype at scales between macro and MEMS, but with rich topologies and material choices one would expect in designing human-scale vehicles. With these challenges in mind, we present progress in the essential technologies for insect-scale robots, or “pico” air vehicles.

## 1 Introduction

Over the past two plus decades there have been multiple research projects aimed at the development of a flapping-wing robotic insect. These include a butterfly-like ornithopter from the University of Tokyo [1], the “Micromechanical Flying Insect” project at U.C. Berkeley [2, 3], and the Harvard “RoboBee” project [4]. These efforts are motivated by tasks such as hazardous environment exploration, search and rescue, and assisted agriculture - similar to the tasks cited for many autonomous robots regardless of scale or morphology. Using swarms of small, agile, and potentially disposable robots for these applications could have benefits over larger, more complex individual robots with respect to coverage and robustness to robot failure. But the interest in these types of robots goes well beyond the expected tasks; use as tools to study open scientific questions (e.g. fluid mechanics of flapping flight, control strategies for computation and sensor limited systems) and the necessary technological achievements that must accompany these projects are the real motivations.

Work in unmanned aerial vehicles has a rich history that spans from scientific inquiry to congressional policy<sup>1</sup>. In 1997, the United States Defense Advanced Re-

---

The authors are with the Harvard School of Engineering and Applied Sciences, 33 Oxford St, Cambridge, MA 02138, e-mail: [rjwood@seas.harvard.edu](mailto:rjwood@seas.harvard.edu)

<sup>1</sup> Section 220 of the National Defense Authorization Act for Fiscal Year 2001 states that, “It shall be the goal of the Armed Forces to achieve the fielding of unmanned, remotely controlled technology such that... by 2010, one-third of the aircraft in the operational deep strike force aircraft fleet are unmanned” [5].

search Projects Agency (DARPA) announced its “micro air vehicle” program which defined an MAV as being 15cm or less in largest linear dimension, have a range of 10km, peak velocities over 13m/s, and operate for more than 20 minutes<sup>2</sup>. Performers in this program developed multiple successful MAV prototypes including the Black Widow and Microbat [6] as well as some of the first examples of piezoelectrically actuated MAVs [7, 2]. In 2005, DARPA again pushed the limits of aerial robotics by announcing the “Nano Air Vehicle” program<sup>3</sup> which had the requirements of 10 gram or less vehicles with 7.5cm maximum dimension, able to fly 1km or more. Results include the 16 cm, 19 gram “Nano Hummingbird” from Aerovironment<sup>4</sup>, the maple seed-inspired Lockheed “Samarai”<sup>5</sup>, and a coaxial helicopter from a Draper Labs led team<sup>6</sup>. There are also a number of recent commercially-available flapping-wing toy ornithopters and RC helicopters on the scale of micro air vehicles such as the Silverlit ‘iBird’ and the Wowwee Flytech toys<sup>7</sup>.

Using these trends, we define a “pico” air vehicle as having a maximum takeoff mass of 500 milligrams or less and maximum dimension of five centimeters or less. This is in the range of most flying insects [8], and thus for pico air vehicles we look primarily to insects for inspiration. An example prototype pico air vehicle, a prototype from the Harvard RoboBee project<sup>8</sup> is shown in Fig. 1.

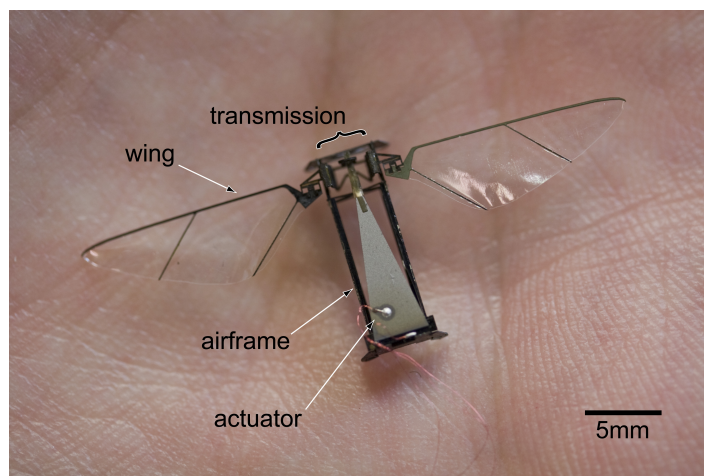


**Fig. 1** Example of a recent prototype of a “RoboBee”. These two-wing, 100 mg robots are capable of controlled thrust and body moments.

<sup>2</sup> <http://www.defense.gov/releases/release.aspx?releaseid=1538>

<sup>3</sup> DARPA BAA-06-06

<sup>4</sup> <http://www.avinc.com/nano/>

<sup>5</sup> <http://www.atl.lmco.com/papers/1448.pdf>

<sup>6</sup> [http://www.draper.com/Documents/explorations\\_summer2010.pdf](http://www.draper.com/Documents/explorations_summer2010.pdf)

<sup>7</sup> <http://www.wowwee.com/en/products/toys/flight/flytech>

<sup>8</sup> <http://robobees.seas.harvard.edu>

Regardless of the classification, the challenges of creating effective flying robots span many disciplines. For example, fluid mechanics changes as a function of characteristic length and velocity: micro air vehicles on the scale of large birds ( $Re > 10,000$ ) exist in a regime of turbulent flow and steady lift to drag ratios greater than 10 [8]. Nano air vehicles may exist in the transition region ( $1000 < Re < 10,000$ ) and thus the impact of boundary layer separation (and potential reattachment) becomes particularly relevant. Whereas for pico air vehicles ( $Re < 3000$ ), the flow is almost entirely laminar and thus so-called *unsteady* mechanisms can be employed to enhance lift beyond what would be achievable from constant velocity alone. Nonetheless, it appears that the energetic cost for flight - when considering a metric similar to cost of transport - increases with decreasing characteristic length. Where we could expect a larger-scale aircraft (tens of meters in characteristic dimension) to stay aloft for many hours or even days, flight times for micro, nano, and pico air vehicles are expected to be on the order of an hour, a few tens of minutes, and less than ten minutes respectively [9].

Similar scaling trends also exist for device manufacturing. It is useful to make a distinction between *feature size* and *characteristic size* as pertaining to a vehicle: the former refers to the smallest dimension of the mechanical components of the system - the pitch of gear teeth, thickness of a constituent material, and length of a flexure are examples - while the latter is more descriptive of the overall scale of the vehicle and can refer to the wingspan, chord length, or some similar quantity. We make the argument that as the characteristic size of a vehicle is reduced, feasible approaches to fabrication and assembly of the various propulsion and control mechanisms makes a distinct transition between more standard approaches using “off-the-shelf” components and machining and assembly tools to requiring entirely novel methods. This is one of the fundamental challenges to creating a pico air vehicle. As the feature sizes of the mechanical components are decreased below around 10-100 microns, the designer can no longer rely on standard macro-scale machining techniques. Even high resolution CNC mills<sup>9</sup>, with positioning accuracy down to one micron require end mills which are rare or non-existent below 50-100 microns. Furthermore, the physics of scaling dictates that as the feature size is decreased, area-dependent forces (e.g. friction, electrostatic, and van der Waals) become dominant, causing more traditional bearing joints to be very lossy with respect to power transmission [10]. Similar arguments can be made for transducers. As the feature size is reduced, friction losses and limits on current density decrease the effectiveness of electromagnetic motors [10]. For example, the induction motor in a Tesla Roadster can produce over 7kW/kg at nearly 90% transduction efficiency<sup>10</sup> whereas the smallest DC motors commercially available can produce 39W/kg at less than 18% efficiency<sup>11,12</sup>. A deeper discussion of actuator geometries and materials

<sup>9</sup> For example, Microlution 5100: <http://microlution-inc.com/products/5100.php>

<sup>10</sup> <http://www.teslamotors.com/roadster/specs>

<sup>11</sup> SBL02-06H1 from Namiki: [http://www.namiki.net/product/dcmotor/pdf/sbl02-06ssd04\\_01\\_e.pdf](http://www.namiki.net/product/dcmotor/pdf/sbl02-06ssd04_01_e.pdf)

<sup>12</sup> Note that this does not include drive circuitry, which is also exacerbated at small scales.

will be presented in Sec. 2.2. Regardless of the transduction mechanism, it is clear that a pico air vehicle will require non-traditional solutions to device fabrication. MEMS (microelectromechanical systems) surface micro machining techniques offer one path to achieve micron-order feature sizes. However, these techniques are hindered by the time-consuming serial nature of the process steps, limited three-dimensional capabilities, and the high cost of prototyping using MEMS foundries. A solution for fabrication and assembly of a pico air vehicle will be described in Sec. 2.4 and examples of both ends of the fabrication spectrum are shown in Fig. 2.

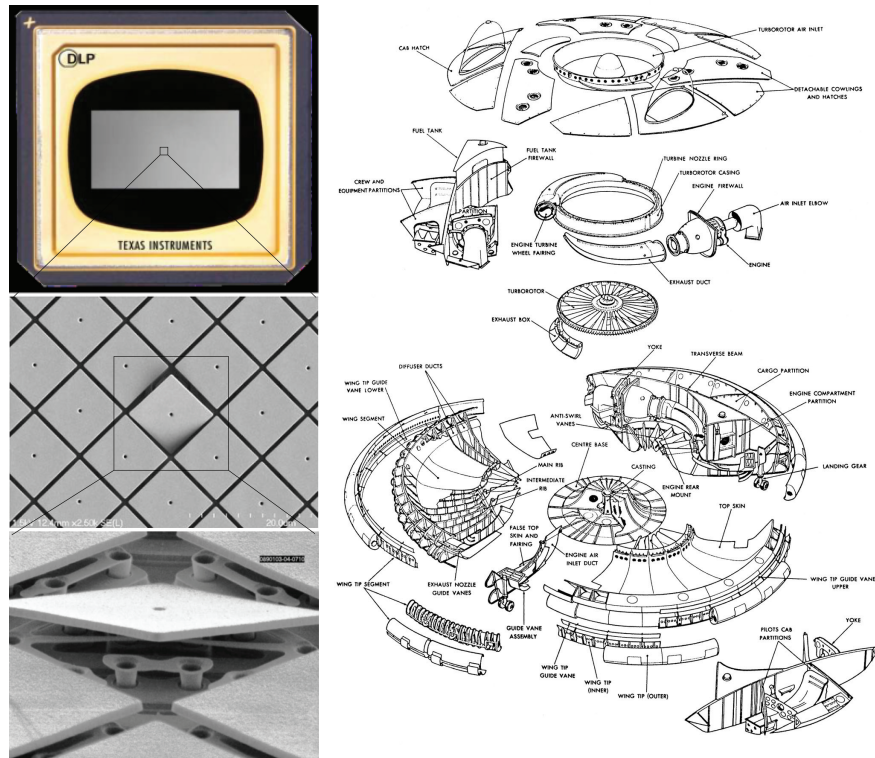


**Fig. 2** At two ends of the fabrication and assembly spectrum: MEMS surface micromachined mirrors from a Texas Instruments DLP display (left, images courtesy of Jack Grimmet and Martin Izzard, Texas Instruments) and a “nuts-and-bolts” approach to assembly of a complex macro-scale device: an experimental “human-scale” hover-capable aircraft, the “Avrocar” [11] (right).

Challenges for control are also scale-dependent. Larger-scale vehicles can take advantage of passive stability mechanisms (e.g. positive wing dihedral) and generally have larger mass and power capacity for various sensors and computer architectures. An insect-scale device will have significantly reduced payload capacity as compared to a micro or even nano air vehicle. Therefore, the control challenges for a pico air vehicle are currently centered around flight stabilization using limited

sensing and computation capabilities. This is in contrast to “higher-level” control problems of autonomous navigation [12] and coordination of multiple unmanned air vehicles [13].

Beyond aeromechanics, actuation, fabrication, and control, there are numerous additional issues including power, system-level design, integration, and mass production. Thus the challenges for a pico air vehicle are daunting, yet form a set of exciting and well-posed engineering questions and scientific opportunities. The remainder of this article will discuss recent progress in a number of these areas.

## 2 Overview of a pico air vehicle

This article will focus on some of the key components of a flapping-wing pico air vehicle, as shown in Fig. 3, based on the design of the Harvard RoboBee. These components make up the majority of the power and mass budget for the pico air vehicle, which is shown in Fig. 4 for a hypothetical 100 milligram robot. Note the dominance of battery and actuator mass and actuator power, which is indicative of the energetic cost of flight at these scales.

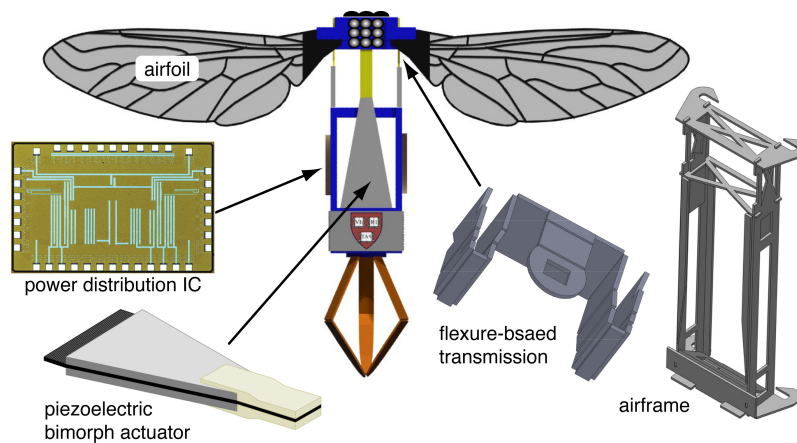


**Fig. 3** Components of a pico air vehicle.

### 2.1 Aeromechanics

Due to scaling of fluid properties, insects operate in a way fundamentally different from conventional aircraft. Although there are many, sometimes subtle, differences between the flight apparatuses of individual species, in general, insects have one or two pairs of wings, driven in multiple rotational degrees of freedom by flight musculature, and powered by metabolic processes which convert chemical energy for

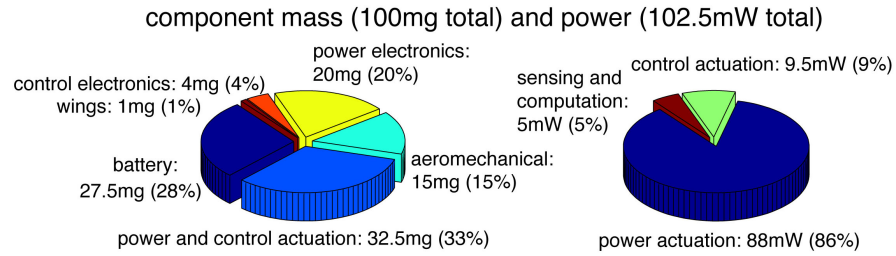


**Fig. 4** Mass (left) and power (right) budgets for a 100 milligram robot, derived using the method in [9].

flight. For a flapping-wing pico air vehicle, we derive some design principles from Dipteran (two-winged) insects. We assume that each wing has two rotational degrees of freedom (DOFs): flapping and rotation about an axis approximately parallel to the leading edge (i.e. pronation and supination). During flapping, the upstroke and downstroke are assumed to be nominally symmetric with no stroke plane deviation. The wing motion is illustrated in Fig. 5. Thinking about the propulsion mechanism as a lumped-parameter 2<sup>nd</sup> order system, the dominant components are the inertia of the wing, potential energy storage in the muscles, plates, and joints of the thorax, and the damping due to interaction between the wing and the air. As with Diptera and other insects which use *indirect* flight muscles, we assume that the wing drive for a flapping-wing pico air vehicle will also operate at resonance to amplify the wing stroke [8].

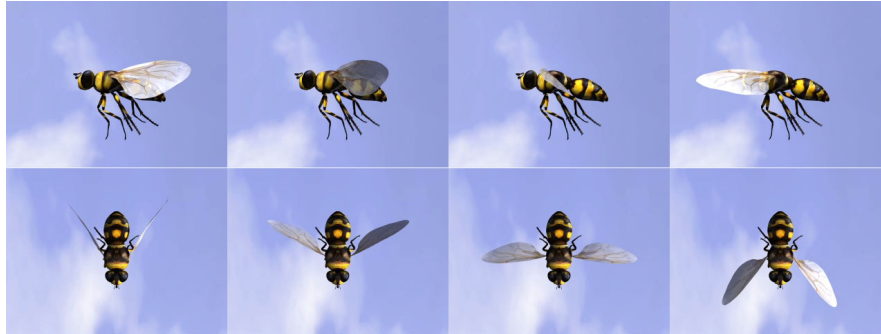


**Fig. 5** Illustration of one-half cycle of wing motion (i.e. the down-stroke) for a Diptera assuming negligible stroke plane deviation. Top row: lateral perspective. Bottom row: dorsal perspective.

In order to control motion in these two DOFs, the actuators are coupled to the wings using a flexure-based articulated transmission mechanism (see Fig. 3). Previous designs utilized a spherical five-bar mechanism to map two linear actuator inputs to the two wing DOFs [14]. Kinematically, this allows direct control over the phasing of wing rotation and any asymmetries in between the upstroke and down-

stroke. However, dynamic coupling between the two degrees of freedom creates challenges for controlled trajectories at the flapping resonant frequency. Instead, an under-actuated version of the transmission includes a passive flexure hinge at the wing base such that flapping is commanded by a single power actuator and rotation is passive [15]. Tuning the dynamics of the system at design time places the rotational resonance well above the flapping resonance such that we can assume quasi-static wing rotation while driving the actuator at the first flapping resonant frequency. There is evidence that wing rotation in some insects is driven by inertial and aerodynamic forces, as opposed to directly activated by thoracic musculature [16, 17, 18].

The presence of unsteady flow features arising from wing-wake and wing-wing interactions, aeroelastic coupling between fluid pressure and wing bending [19, 20], and the significance of vortex formation and shedding [21] result in challenges for a succinct description of the relationship between wing properties (geometric, inertial, and elastic), wing motions and deformation, and resulting flow and force generation. To study the aeromechanics of flapping-wing flight, researchers have employed a variety of methods including dynamic scaling [21], computational fluid dynamics (CFD) methods [22], and direct biological observation [23]. Each of these has led to significant insights into the details of flow structure, performance of many flying insects, and the function of various morphological features. A combination of these methods, the *blade-element* method [24], merges quasi-steady flow analysis with empirically-fit force and torque coefficients which hide all the unsteady terms behind these coefficients. This has allowed designers to study a variety of wing morphologies and trajectories. However, in some cases, the aeroelastic interaction between strain energy in the airfoil and fluid pressure may have a non-negligible effect on the dynamics and energetics of the vehicle. In such cases, it is valuable to study the fluid mechanics using either a moving-mesh CFD code or at-scale experiments which do not make any scaling assumptions on wing compliance.

Given the ability to manufacture insect-scale airfoils, such as the *Eristalis* wing in Fig. 6 [25], and actuate with insect-like trajectories and wingbeat frequencies, we have begun multiple experiments which are aimed at a deeper understanding of the fluid mechanics for a pico air vehicle with emphasis on learning design rules to enhance aerodynamic efficiency - and thus overall performance of the robot. Recent experiments include:

- Multiple methods to create biomimetic airfoils and verification that the static characteristics are consistent with biological wings [26, 25].
- Established a blade-element based model of under-actuated flapping dynamics (i.e. passive rotation) and validated using a custom-made single flapping-wing, high resolution force sensing [27], and high speed motion reconstruction [24].
- Explored the function of distributed vs localized wing compliance on lift force generation [28].



**Fig. 6** Photo of a micromolded polymer wing mimicking the features of a *Eristalis* wing (top). This wing was created in a single molding step and includes veins ranging from  $50\text{-}125\mu\text{m}$  thick,  $100\mu\text{m}$  corrugation, and a  $10\text{-}20\mu\text{m}$  membrane. A sample of the wing motion (dorsal perspective) at  $150\text{Hz}$  flapping frequency taken from a high speed video (bottom).

## 2.2 Actuation

As previously discussed, the physics of scaling requires us to seek an alternative to electromagnetic actuation for a pico air vehicle. But there are more subtle reasons for this as well. Even if the power densities and efficiencies were comparable, the unloaded RPM of a rotary electromagnetic motor will typically increase with decreasing size, thus requiring substantial gearing to produce useful work and increasing the overall complexity of the transmission system. Furthermore, as we are assuming a reciprocating flapping motion, a rotary motor would require additional transmission components (and rotary bearings) to convert the rotation to wing flapping, again increasing part count and complexity. Instead we look to oscillatory actuators based on induced-strain materials. Induced-strain materials respond to an applied stimulus with a simple change in geometry. There are multiple options including piezoelectric, electroactive polymers, solid-state phase transitions, electrostriction, and thermal expansion. There have also been many demonstrations of relatively simple geometries for producing linear actuation from electrostatic forces [29], clever piezoelectric linear motors<sup>13</sup>, piezoelectric stacks and “moonie” type actuators [30], and many dielectric elastomer configurations [31]. Each material and actuator morphology can be evaluated based on the standard metrics of blocked force, free displacement (and thus energy), density (and thus energy density), band-

<sup>13</sup> “Squiggle” motors: [http://www.newscaletech.com/squiggle\\_overview.html](http://www.newscaletech.com/squiggle_overview.html)

**Table 1** Qualitative comparison of actuation technologies.

●=highest, ●=high, ◐=moderate, ◑=low, ○=lowest

type	example	efficiency	toughness	bandwidth <sup>1</sup>	max. $\epsilon$	max. $\sigma$	density
bulk piezo.	PZT-5H <sup>2</sup>	◐	◐	●	○	◐	●
single crystal	PZN-PT <sup>3</sup>	◐	○	●	◐	◐	●
SMA	Nitinol <sup>4</sup>	○	◐	◐	◐	●	●
IPMC	Nafion <sup>5</sup>	◐	◐	◐	●	◐	◐
EAP	DE <sup>6</sup>	◐	◐	◐	●	◐	◐
electromag.	brushless <sup>7</sup>	◐	NA	◐	NA	NA	●

<sup>1</sup> depends upon structure geometry

<sup>2</sup> from Piezo Systems: <http://www.piezo.com>

<sup>3</sup> single crystal piezoelectric ceramics, see [33]

<sup>4</sup> shape memory alloy: <http://www.dynalloy.com>

<sup>5</sup> from DuPont, see [34]

<sup>6</sup> dielectric elastomers, see [31]

<sup>7</sup> for example, 0308 DC micro-motor from Smoovy: <http://www.faulhaber-group.com>

width (and thus power density), and efficiency. However, the focus is not only on performance, but also practicality. Therefore, additional considerations include fabrication complexity, cost, robustness, the drive method, and linearity of the input-output response and any related control issues. Table 1 qualifies actuation options relative to some of these metrics. A more comprehensive study of actuation choices for a pico air vehicle is presented in [32] with reference to multiple flapping-wing design break points.

Given the needs of a pico air vehicle, we chose clamped-free bending bimorph polycrystalline piezoelectric actuators as a local minimum in complexity while meeting the key specifications for bandwidth, power density, and efficiency. Furthermore, we can rapidly prototype many geometries and obtain all necessary materials commercially. Note that the use of these piezoelectric actuators also carries some important scaling decisions since we are assuming a resonant primary drive. The resonant frequency will monotonically increase with decreasing size (this trend can be seen clearly in insects [8]). For quasi-static operation of the piezoelectric actuators, the power density will increase roughly linearly with operating frequency. Thus for smaller devices, this type of actuator is attractive and can outperform insect flight muscle by a factor of two or more [35]. The opposite trend is true as well: it is clear that, for direct-drive transmissions, above a certain size these actuators will not be able to deliver sufficient power due to a fixed (either fracture or breakdown-limited) energy density and reduced operating frequencies. The specific cutoff is highly dependent on the details of the vehicle design and will not be discussed here. Finally, we do not assume that piezoelectric actuation is the best choice for all functions of a pico air vehicle. As discussed in Sec. 2.3, we divide actuation between

power delivery and control. The previous discussions have focused on maximizing resonant power delivery in order to generate thrust to maintain flight, however the requirements for a control actuator could be rather different than a power actuator, thus a hybrid solution is a potentially viable option.

### 2.3 Control

The challenges for control for a pico air vehicle are not in planning and navigation, but rather more fundamental topics of stabilization, sensing, and electromechanical design. Flapping-wing robots similar to the one in Fig. 1 are designed such that the mean lift vector passes through the center of mass and the periodic drag forces are symmetric on the upstroke and downstroke, thus there are nominally zero body torques during flight. However, fabrication errors and external disturbances can easily excite instabilities in the roll, pitch, or yaw angles which need to be actively suppressed. Fig. 7 displays a typical behavior in the absence of any controller or constraints on the body degrees of freedom for a flapping-wing pico air vehicle. It is worth noting that the robot in Fig. 7 survived over ten such crashes without any damage, which demonstrates the robustness of the materials and components that constitute the robot.

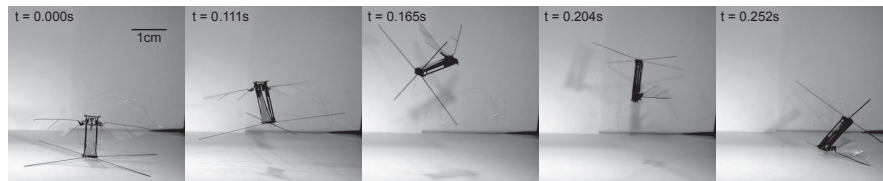


**Fig. 7** When driven open-loop, the RoboBee prototypes are very unstable in body rotations and crash shortly after takeoff.

Our control efforts to date have concentrated on (a) development of the thoracic mechanics to enable modulation of wing trajectories and hence body torques, (b) exploration of appropriate sensor technologies, and (c) methodologies for controller synthesis and related demonstrations. Recent progress in these areas include:

- We have demonstrated the ability to generate lift greater than body mass and perform uncontrolled takeoff experiment such as shown in Fig. 7 [4]. This provides the baseline aeromechanical design and allows us to quantify the thrust the robot can achieve to help bound payload for sensing and power.
- The original designs presented in [4] only had the ability to control thrust and one body torque (i.e. pitch torques). We have demonstrated the ability to generate bilateral asymmetry in stroke amplitude using multiple thoracic mechanics configurations [36, 37]. This involves a morphological separation of power and control actuation similar to the role of the *indirect* and *direct* flight muscles in the thoracic mechanics of Dipteran insects [38].

- Similarly, we have performed experiments with stroke plane deviation as an alternative method for torque generation in [39].
- Beyond modulating the wing trajectory, we have performed torque measurement experiments which verify that there is a one-to-one relationship between dorso-ventral mean stroke angle bias and the resulting pitch torque [40].
- Through collaborations with Centeye, Inc<sup>14</sup>, insect-inspired optical flow sensors have been integrated on-board a gliding micro air vehicle [41].
- Work at U.C. Berkeley has prototyped a number of insect-inspired inertial and horizon-detection sensors such as a biomimetic haltere (similar to the Coriolis force sensing structures in Diptera [42]) and photoreceptive ocelli similar to the horizon detection sensors in insects [43].
- Finally, we have implemented an adaptive control scheme to control the mean lift force during flapping [44].

These efforts are primarily focused on the standard feedback control strategy in which a disturbance is detected by a proprioceptive sensor, a computer chooses a compensatory action according to some control law, and the action is then implemented by a system of amplifiers and electromechanical structures. We refer to devices which perform such complex tasks without the intervention of electrical circuits (i.e. analog or digital computers) as examples of *mechanical intelligence*. There are many everyday examples including windshield wipers, whippletrees, and automobile differentials. In these examples, feedback control is performed as a consequence of the mechanical design. For example, automobile differentials automatically distribute equal torques to the wheels regardless of differences in wheel velocities. We have applied this concept to the passive regulation of wing motions by a modified version of the flexure-based transmission called PARITY: “Passive Aeromechanical Regulation of Unbalanced Torques” [45]. The PARITY design equally distributes torques to the wings in response to perturbations, due to either external disturbances or fabrication errors, without the need for sensors or computation. This allows an active controller to operate on a much longer time scale since short time scale perturbations are eliminated, thereby reducing the required sensor bandwidth and computation power.

## 2.4 Fabrication

The integrated circuit revolution of the 1950s and 1960s now enables the majority of the consumer electronics that are enjoyed daily. As these techniques evolved in the 1980s to include electromechanical components, an even greater space of applications emerged including sensors, optics, and even actuation [46]. Microrobots have been made using MEMS surface and bulk micromachining techniques [47, 48]. However, there are many drawbacks to using integrated circuit (IC) and MEMS technologies to create a pico air vehicle. First is the dramatic difference between the material properties of silicon and insect tissue: the former being rigid and brittle

---

<sup>14</sup> <http://www.centeye.com>

while the latter exhibits a large range of material properties, is generally quite resilient, and is approximately the density of water. Second, although the suite of techniques for high resolution machining is an appealing aspect of MEMS processes, the resulting structures are typically “2.5D”, with high aspect ratio components being extremely challenging in terms of machining or requiring hinged structures [49]. Finally, although MEMS foundries exist (e.g. the Multi-User MEMS Process, MUMPS<sup>15</sup> and Sandia’s SUMMiT<sup>16</sup>), cost and turnaround time are generally prohibitive to rapid prototyping. With the advent of *mesoscopic* manufacturing methods [50], we have demonstrated key components of the flight apparatus of robotic insects [51, 15] and recently the first demonstration of a 60 milligram flapping-wing device which can produce thrust greater than its body weight [4] has proven the feasibility of creating insect-scale flying robots using these techniques.

Mesoscopic manufacturing based on lamination and folding is depicted in Fig. 8. Here a spherical five-bar mechanism is created in three steps. First, the constituent materials - typically thin sheets of polymers, metals, ceramics, or composites - are laser micromachined to the desired planform geometries. These layers are then aligned and laminated using thermoset sheet adhesives and a heated press. Second, the quasi-planar devices are released using a final laser machining step. Lastly, the devices are folded into their final configuration. In the case in Fig. 8, tabs and slots are integrated to assist with alignment during folding, although there are other methods to ensure precision in this final step including fixturing, surface tension, differential thermal expansion, and even embedded actuation [52]. This process enables the development of articulated components with any number of DOFs, layered actuators such as the piezoelectric bending actuators described in Sec. 2.2, and integrated electronics, all with feature sizes ranging from micron to centimeter. The concept of folding as an assembly process has been further developed into the a larger space of applications for “Programmable Matter” using robotic origami to produce arbitrary shapes and functional structures [53].

## 2.5 Power

The power source for a pico air vehicle is the most significant delimiter to flight time [9]. Options for power storage include electrochemical (i.e. batteries and fuel cells [54]), electrostatic (i.e. capacitors and supercapacitors), and mechanical (i.e. elastic strain energy)<sup>17</sup>. As with all components, practicality is a fundamental consideration. Existing batteries have poor energy storage (approximately 500J/g based on existing small-scale lithium batteries from Fullriver<sup>18</sup>) compared to fuels such as gasoline which can be two orders of magnitude greater. But energy density alone is not sufficient to describe the effectiveness of a candidate power source. Conversion efficiency, storage/packaging, and operating conditions should also be considered.

---

<sup>15</sup> <http://www.memscapinc.com>

<sup>16</sup> <http://www.mems.sandia.gov/tech-info/summit-v.html>

<sup>17</sup> Note that this only refers to storage, not transduction or harvesting.

<sup>18</sup> <http://www.fullriver.com/>

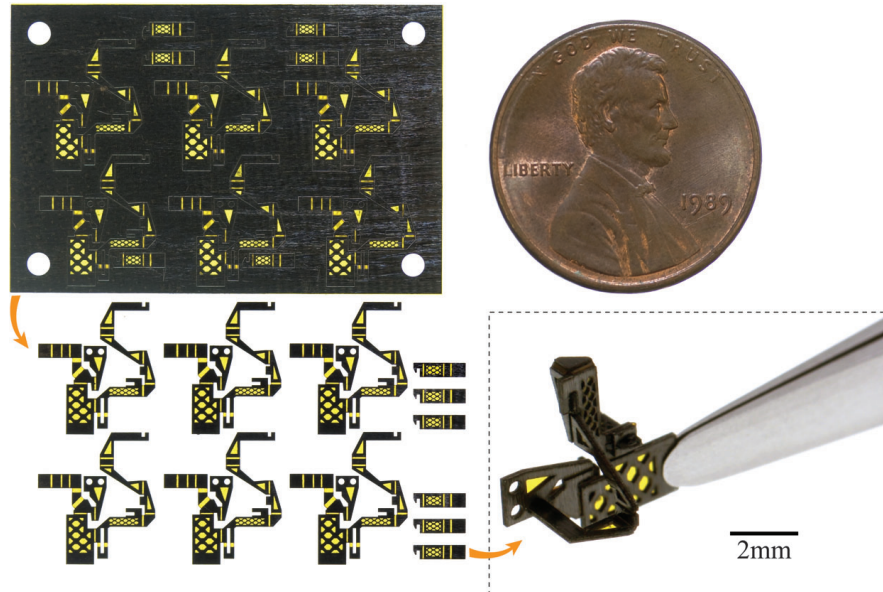


**Fig. 8** Example of the process flow for articulated microstructures. In this example, six spherical five-bar linkages are created by a sequential micromachining and lamination process, then folded into the final configuration (inset).

There are sub-gram batteries which are commercially available<sup>18</sup>. While the lower end of this range (approximately 200mg) could be acceptable for a pico air vehicle, smaller batteries are feasible, though rare or non-existent as commercial products. Since the electrochemical reactions are scale-independent (at least for the scales considered here), creating smaller batteries becomes an exercise in fabrication and packaging. For example, it is possible to dice and repackage lithium-polymer batteries in an inert atmosphere.

Power distribution efficiency is also a fundamental concern. Assuming the source will have a voltage of approximately 3.7V, and using the piezoelectric actuator dimensions from [51], the power distribution circuits for a pico air vehicle will require a boost conversion stage with a step-up ratio in the range of 50-100 [55]. Options for boost conversion include piezoelectric transformers, charge pump ladder circuits, and electromagnetic transformers. Once the source voltage is boosted to the proper level, the actuator drive signal is generated. Considering the low electromechanical coupling coefficients for many piezoelectric materials, it is essential to recover remaining charge from one half cycle of the harmonic oscillation of the thorax and use for the next half cycle. Charge recovery circuits for bimorph actuators have been developed [56] and a custom integrated circuit which generates the periodic drive signal and coordinates charge recovery has been created and demonstrated for a flapping-wing robot [57]. Therefore, the power source is the key remaining technology required to bring the pico air vehicle in Fig. 1 to power autonomy.

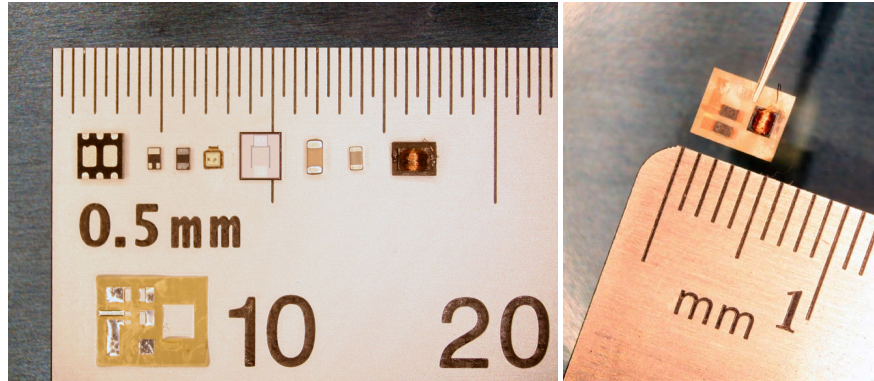


**Fig. 9** Components (left) and a complete tapped-inductor-based 20 milligram boost conversion circuit (right).

### 3 Next steps

The progress on pico air vehicles reported in this article is the tip of the iceberg. The next steps include:

- **Power source:** Characterization of batteries and other viable power sources (including supercapacitors and micro fuel cells) under appropriate loading conditions.
- **Integration:** The best demonstration for any core technology involves integration onto a flight-worthy robot.
  - *On-board sensors:* Continued collaboration with manufacturers of optical flow sensors (Centeye, Inc.), aiming to demonstrate a flight-worthy sensor and use in altitude control experiments.
  - *On-board power electronics:* Integrating the components from Fig. 9 into the airframe utilizing the layered manufacturing technique described in Sec. 2.4.
- **Accelerator-based computation:** The RoboBees project is exploring compute architectures which employ highly specialized integrated circuits to perform a single task (such as control or sensor processing) extremely efficiently.
- **System-level design and optimization:** Finally, while much attention has been paid to each component, there has been few efforts for system-level optimization for vehicles of this scale. The work in [9] suggests the most promising areas to focus design efforts and how improvements to the performance of any subsystem will contribute to increased flight time.

**Acknowledgements** This work was partially supported by the National Science Foundation (award number CCF-0926148), the Army Research Laboratory (award number W911NF-08-2-0004), the Office of Naval Research (award number N00014-08-1-0919-DOD35CAP), and the Air Force Office of Scientific Research (award number FA9550-09-1-0156-DOD35CAP). Any opin-

ions, findings, and conclusions or recommendations expressed in this material are those of the authors and do not necessarily reflect the views of the National Science Foundation.

## References

1. H. Tanaka, K. Hoshino, K. Matsumoto, I. Shimoyama, in *IEEE/RSJ Int. Conf. on Intelligent Robots and Systems* (Edmonton, Alberta, Canada, 2005)
2. R. Fearing, K. Chang, M. Dickinson, D. Pick, M. Sitti, J. Yan, in *IEEE Int. Conf. on Robotics and Automation* (2000)
3. R. Fearing, S. Avadhanula, D. Campolo, M. Sitti, J. Yan, R. Wood, in *Neurotechnology for Biomimetic Robots* (The MIT Press, 2002), pp. 469–480
4. R. Wood, *IEEE Transactions on Robotics* **24**(2) (2008)
5. National Defense Authorization Act, Fiscal Year 2001 (2000). Public Law 106-398, 106<sup>th</sup> Congress
6. M. Keenmon, J. Grasmeyer, in *AIAA/ICAS Intl. Air and Space Symp. and Exposition: The Next 100 Years* (Dayton, OH, 2003)
7. A. Cox, D. Monopoli, D. Cveticanin, M. Goldfarb, E. Garcia, in *J. of Intelligent Material Systems and Structures*, vol. 13 (2002), vol. 13, pp. 611–615
8. R. Dudley, *The Biomechanics of Insect Flight: Form, Function and Evolution* (Princeton University Press, 1999)
9. M. Karpelson, J. Whitney, G.Y. Wei, R. Wood, in *IEEE/RSJ Int. Conf. on Intelligent Robots and Systems* (Taipei, Taiwan, 2010)
10. W. Trimmer, *J. of Sensors and Actuators* **19**, 267 (1989)
11. Avro Canada VZ-9AV Avrocar (2010). <http://www.nationalmuseum.af.mil/factsheets/factsheet.asp?id=10856>
12. S. Shen, N. Michael, V. Kumar, in *IEEE Int. Conf. on Robotics and Automation* (Shanghai, China, 2011)
13. T. Stirling, D. Floreano, in *Proceedings of the 10th International Symposium on Distributed Autonomous Robotics Systems*. (2010)
14. S. Avadhanula, R. Wood, D. Campolo, R. Fearing, in *IEEE Int. Conf. on Robotics and Automation* (Washington, DC, 2002)
15. R. Wood, in *IEEE/RSJ Int. Conf. on Intelligent Robots and Systems* (San Diego, CA, 2007)
16. A. Ennos, *J. of Experimental Biology* **140**, 161 (1988)
17. A. Ennos, *J. of Experimental Biology* **140**, 137 (1988)
18. A. Bergou, S. Xu, Z. Wang, *Journal of Fluid Mechanics* **591**, 321 (2007)
19. S. Combes, T. Daniel, *J. of Experimental Biology* **206**(17), 2989 (2003)
20. S. Combes, T. Daniel, *J. of Experimental Biology* **206**(17), 2999 (2003)
21. M. Dickinson, F.O. Lehmann, S. Sane, *Science* **284**, 1954 (1999)
22. R. Mittal, G. Iaccarino, *Ann. Rev. Fluid Mechanics* **37**, 239 (2005)
23. C. Ellington, C. van der Berg, A. Willmott, A. Thomas, *Nature* **384**, 626 (1996)
24. J. Whitney, R. Wood, *J. Fluid Mechanics* **660**, 197 (2010)
25. H. Tanaka, R. Wood, *J. Micromechanics and Microengineering* **20**(7) (2010)
26. J. Shang, S. Combes, B. Finio, R. Wood, *Bioinspir. Biomim.* **4**(036002) (2009)
27. R. Wood, K.J. Cho, K. Hoffman, *J. Smart Materials and Structures* **18**(125002) (2009)
28. H. Tanaka, J. Whitney, R. Wood, *J. Integrative & Comparative Bio.* **51**(1), 142 (2011)
29. W. Tang, T.C. Nguyen, M. Judy, R. Howe, *J. of Sensors and Actuators A: Physical* **21**(1–3), 328 (1990)
30. R. Newnham, A. Dogan, Q. Xu, K. Onitsuka, J. Tressler, S. Yoshikawa, in *Proc. IEEE Ultrasonics Symp.*, vol. 1 (Baltimore, MD, 1993), vol. 1, pp. 509–513
31. R. Pelrine, P. Sommer-Larsen, R. Kornbluh, R. Heydt, G. Kofod, Q. Pei, P. Gravesen, in *Proc. of Int. Soc. Opt. Eng.*, vol. 4329 (2001), vol. 4329, pp. 335–349
32. M. Karpelson, G.Y. Wei, R. Wood, in *IEEE Int. Conf. on Robotics and Automation* (Pasadena, CA, 2008)

33. J. Yin, B. Jiang, W. Cao, *IEEE Trans. on Ultrasonics, Ferroelectrics, and Frequency Control* **47**(1), 285 (2000)
34. S. Lee, H. Park, K. Kim, *Smart Materials and Structures* **14**(6), 1363 (2005)
35. E. Steltz, R. Fearing, in *IEEE/RSJ Int. Conf. on Intelligent Robots and Systems* (San Diego, CA, 2007)
36. B. Finio, J. Shang, R. Wood, in *IEEE Int. Conf. on Robotics and Automation* (Kobe, Japan, 2009), pp. 3449–3456
37. B. Finio, B. Eum, C. Oland, R. Wood, in *IEEE Int. Conf. on Robotics and Automation* (St. Louis, MO, 2009)
38. B. Finio, R. Wood, *Bioinspir. Biomim.* **5**, 045006 (2010)
39. B. Finio, J. Whitney, R. Wood, in *IEEE/RSJ Int. Conf. on Intelligent Robots and Systems* (Taipei, Taiwan, 2010)
40. B. Finio, K. Galloway, R. Wood, in *IEEE/RSJ Int. Conf. on Intelligent Robots and Systems* (San Francisco, CA, 2011)
41. R. Wood, S. Avadhanula, E. Steltz, M. Seeman, J. Entwistle, A. Bachrach, G. Barrows, S. Sanders, R. Fearing, *Robotics and Automation Magazine* **14**(2), 82 (2007)
42. G. Nalbach, *J. of Comparative Physiology A* **173**, 293 (1993)
43. W. Wu, L. Schenato, R. Wood, R. Fearing, in *IEEE Int. Conf. on Robotics and Automation* (Taipei, Taiwan, 2003)
44. N. Pérez-Arancibia, J. Whitney, R. Wood, in *American Controls Conf.* (San Francisco, CA, 2011)
45. P. Sreetharan, R. Wood, *J. Mechanical Design* **132**(5), 051006 (2010)
46. K. Petersen, *Proc. of IEEE* **70**(5), 420 (1982)
47. R. Yeh, E. Kruglick, K. Pister, *J. of Microelectrical Mechanical Systems* **5**(1), 10 (1996)
48. B. Donald, C. Levey, C. McGray, I. Paprotny, D. Rus, *J. of Microelectrical Mechanical Systems* **15**(1), 1 (2006)
49. K. Pister, M. Judy, S. Burgett, R. Fearing, *J. of Sensors and Actuators A: Physical* **33**, 249 (1992)
50. R. Wood, S. Avadhanula, R. Sahai, E. Steltz, R. Fearing, *J. of Mech. Design* **130**(5) (2008)
51. R. Wood, E. Steltz, R. Fearing, *J. of Sensors and Actuators A: Physical* **119**(2), 476 (2005)
52. J. Paik, E. Hawkes, R. Wood, *J. of Smart Materials and Structures* **19**(12), 125014 (2010)
53. E. Hawkes, B. An, N. Benbernou, H. Tanaka, S. Kim, E. Demaine, D. Rus, R. Wood, *Proc. of the National Academy of Sciences* **107**(28), 12441 (2010)
54. M. Tsuchiya, B. Lai, S. Ramanathan, *Nature Nanotechnology* **6**(282) (2011)
55. E. Steltz, M. Seeman, S. Avadhanula, R. Fearing, in *IEEE/RSJ Int. Conf. on Intelligent Robots and Systems* (Beijing, China, 2006)
56. D. Campolo, M. Sitti, R. Fearing, *IEEE Trans. on Ultrasonics, Ferroelectrics and Frequency Control* **50**(3), 237 (2003)
57. M. Karpelson, R. Wood, G.Y. Wei, in *Symp. on VLSI Circuits* (Kyoto, Japan, 2011)